Article

# Dispersion without Many-Body Density Distortion: Assessment on Atoms and Small Molecules

Derk P. Kooi,* Timo Weckman,* and Paola Gori-Giorgi*

Read Online

ACCESS | Metrics & More | Article Recommendations | Supporting Information

**ABSTRACT:** The "fixed diagonal matrices" (FDM) dispersion formalism [Kooi, D. P.; et al. *J. Phys. Chem. Lett.* **2019**, *10*, 1537] is based on a supramolecular wave function constrained to leave the diagonal of the many-body density matrix of each monomer unchanged, reducing dispersion to a balance between kinetic energy and monomer–monomer interaction. The corresponding variational optimization leads to expressions for the dispersion energy in terms of the ground-state pair densities of the isolated monomers only, providing a framework to build new approximations without the need for polarizabilities or virtual orbitals. Despite the underlying microscopic real space mechanism being incorrect, as in the exact case there is density relaxation, the formalism has been shown to give extremely accurate (or even exact) dispersion coefficients for H and He. The question we answer in this work is how accurate the FDM expressions can be for isotropic and anisotropic $C_6$ dispersion coefficients when monomer pair densities are used from different levels of theory, namely Hartree–Fock, MP2, and CCSD. For closed-shell systems, FDM with CCSD monomer pair densities yield a mean average percent error for isotropic $C_6$ dispersion coefficients of about 7% and a maximum absolute error within 18%, with a similar accuracy for anisotropies. The performance for open-shell systems is less satisfactory, with CCSD pair densities performing sometimes worse than Hartree–Fock or MP2. In the present implementation, the computational cost on top of the monomer's ground-state calculations is $O(N^4)$. The results show little sensitivity to the basis set used in the monomer's calculations.

Dispersion coefficients with different pair densities
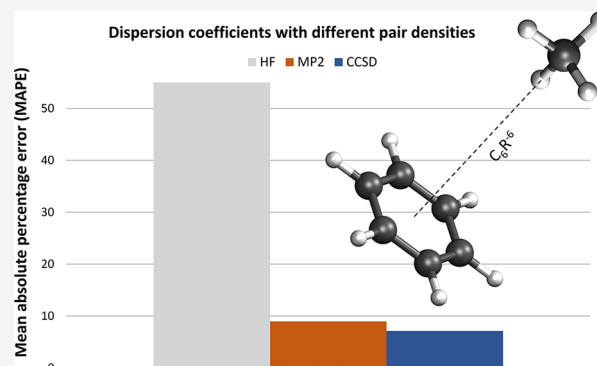
## 1. INTRODUCTION

The attractive London dispersion interaction between atoms and molecules is weaker than covalent bonding forces, but while the latter decay exponentially with the separation $R$ between the monomers, dispersion interactions decay only polynomially in $1/R$. Because of this dominating long-range character, dispersion plays a crucial role in various chemical systems and processes, such as protein folding, soft solid state physics, gas–solid interfaces, etc. An accurate, computationally efficient, and fully nonempirical treatment of dispersion forces remains an open challenge, and it is the objective of several ongoing efforts (see, e.g., refs 1−3 for recent reviews and benchmarks).

We have recently introduced a class of variational wave functions that capture the long-range interactions between two quantum systems without deforming the diagonal of the many-body density matrix of each monomer.[4] The variational take on dispersion is certainly not new, as, for example, variational calculations of the dispersion coefficients have been performed in the context of (Hylleraas) variational perturbation theory[5] and variational calculations of the dispersion energy at finite intermonomer distance have been carried out in the framework of symmetry-adapted perturbation theory (SAPT) using orthogonal projection.[6] The distinctive feature of our approach is the reduction of dispersion to a balance between kinetic energy and monomer–monomer interactions only, providing an explicit expression for the dispersion energy in terms of the ground-state pair densities of the isolated monomers.

Although the supramolecular wave function constructed in this "fixed diagonal matrices" (FDM) approach can never be exact, as density distortion is prohibited, it provides a variational expression for the dispersion energy when accurate pair densities for the momoners are used, at a computational cost given essentially by the ground-state monomer calculations. The FDM approach has been found to yield exact results for the dispersion coefficients up to $C_{10}$ for the H–H case (and up to $C_{30}$ for the second-order coefficients), and very accurate results (0.17% error on $C_6$) for He–He and He–H.[4] This is achieved by reshuffling the contributions of kinetic energy and potential energy inside each monomer, as shown in Table 1 of ref 7. Another way to look at it is the following: dispersion between
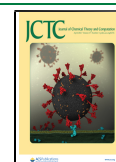
two systems in their ground states is a competition between a distortion of the fragments' ground states (which raises the energy with respect to $E_0^A + E_0^B$) and the interfragment interaction that can lower the energy of the two systems together. As proven by Lieb and Thirring,[8] the rise in energy due to the distortion of the fragments' ground states can be always made quadratic with respect to a set of variational parameters, with the interfragment interaction being linear. With our FDM constraint we force the quadratic rise in energy of the isolated fragments to be of kinetic energy origin only, since only the off-diagonal elements of the monomer's reduced density matrices are allowed to change. For the special case of two ground-state one-electron fragments, this can be shown to give the same result for the dispersion coefficients as second-order Rayleigh–Schrödinger perturbation theory.[7]

This FDM construction is fundamentally different from approaches to incorporate dispersion based on the adiabatic connection (AC) and the fluctuation dissipation theorem (see, for example, ref 9 and references therein). In these methods the interacting system is connected to a noninteracting one with the same density via the AC formalism: the monomer's pair density changes as the electron–electron interaction is turned on. A different AC approach in which only the monomer–monomer interaction is turned on has been introduced very recently in ref 10: the main difference from our FDM formalism is that in our case we keep the densities (and pair densities) of the monomers equal to their isolated ground-state values, while in ref 10 the density is kept equal to the one of the complex for all coupling strength values.

The FDM expressions for the dispersion energy in terms of the ground-state pair densities of the isolated monomers offer a neat theoretical framework to build new approximations, by using pair densities from different levels of accuracy, including exchange–correlation holes from density functional theory. This idea is similar in spirit to the exchange dipole moment (XDM) of Becke and Johnson,[11,12] with the main difference that in our case we do not need the static atomic polarizabilities, as everything can be expressed in terms of ground–state monomer densities and exchange–correlation holes, with a clear supra-molecular variational wave function behind our expressions.[7] Another related approach is the "weighted" exchange-hole (WXhole) idea,[13] in which an approximation for the frequency dependence of the response function is used in order to perform the frequency integration. Again, this is not needed in the FDM approach, which is based on ground-state quantities only.

Besides a route for DFT-based approximations, the FDM idea has the advantage of providing not only energetics but also a simplified supramolecular wave function that can be used in other contexts, for example, in a QM/MM framework to model interactions between the QM and MM parts, following the ideas of refs 14–16 and using results for the functional derivative of the FDM dispersion energy reported in ref 7.

Before considering the use of the FDM framework to build DFT-based approximations or other kinds of models, one should ask the fundamental question: how accurate can this approach be if we use accurate monomer's ground-state pair densities, beyond the simple H and He cases? In other words, how accurate can the FD construction be if we eliminate the other sources of error? The aim of this work is exactly to answer to this question by exploring the performance of the FDM expression for the dispersion $C_6$ coefficient for atoms and molecules using different levels of theory for the monomer calculations, studying the convergence and basis set dependence

of the results. We test the approach on 459 pairs of atoms, ions, and small molecules, using Hartree–Fock (HF), second-order Møller–Plesset perturbation theory (MP2), and coupled cluster with singles and doubles (CCSD) ground-state pair densities. We should keep in mind that the FDM expression is guaranteed to be variational, yielding a lower bound to $C_6$, only when we use exact pair densities of the monomers. As we shall see, for closed-shell systems, this is almost always the case with CCSD pair densities, which yield in general good results, slightly under-estimating $C_6$, although there are exceptions. With HF pair densities, as it was already found in a preliminary result for the Ne–Ne case in ref 4, $C_6$ is, in the vast majority of cases, overestimated.

The paper is organized as follows. In section 2 we illustrate our working equations, including the expressions for the isotropic $C_6$ coefficients and for the anistropies, with the computational details reported in section 3. The results are discussed in section 4, and conclusions and perspectives are in section 5.

## 2. THEORY

We consider two systems $A$ and $B$ separated by a (large) distance $R$ having isolated ground-state wave functions $\Psi_0^A(\underline{\mathbf{x}}_A)$ and $\Psi_0^B(\underline{\mathbf{x}}_B)$, where $\mathbf{x}$ denotes the spin-spatial coordinates $(\mathbf{r}, \sigma)$ and $\underline{\mathbf{x}}_{A/B}$ denote the whole set of the spin-spatial coordinates of electrons in system $A/B$. The FDM framework[4] is defined by the following constrained minimization problem[4,7]

$$E_{\text{disp}}^{\text{FDM}}(R) = \min_{\Psi_R \to |\Psi_0^A|^2, |\Psi_0^B|^2} \langle \Psi_R | \hat{T} + \hat{V}_{ee}^{AB} | \Psi_R \rangle - T_0^A - T_0^B$$
$$- U[\rho_0^A, \rho_0^B] \tag{1}$$

where $\hat{T}$ is the usual kinetic energy operator acting on the full set of variables $\underline{\mathbf{x}}_A, \underline{\mathbf{x}}_B$, and

$$\hat{V}_{ee}^{AB} = \sum_{i \in A, j \in B} \frac{1}{|\mathbf{r}_i - \mathbf{r}_j|}$$

With $T_0^{A/B}$ we denote the ground-state kinetic energy expect-ation values of the two separated systems and

$$U[\rho_0^A, \rho_0^B] = \int d\mathbf{r} \int d\mathbf{r}' \frac{\rho_0^A(\mathbf{r}) \, \rho_0^B(\mathbf{r}')}{|\mathbf{r} - \mathbf{r}'|} \tag{2}$$

where $\rho_0^{A(B)}$ are the ground-state one-electron densities of the two systems. The constraint $\Psi_R \to |\Psi_0^A|^2, |\Psi_0^B|^2$ means that the search in eq 1 is performed over wave functions $\Psi_R(\underline{\mathbf{x}}_A, \underline{\mathbf{x}}_B)$ that leave the diagonal of the many-body density matrix of each fragment unchanged with repect to the ground-state isolated value. We work in the polarization approximation, in which the electrons in $A$ are distinguishable from those in $B$. The constrained-search formulation, eq 1, makes dispersion a simple competition between kinetic energy and monomer–monomer interaction, as all the other monomer energy components cannot change by construction. This also guarantees that no electrostatic or induction contributions appear in eq 1.

For the minimizer of eq 1 we use the variational ansatz of ref 4

$$\Psi(\underline{\mathbf{x}}_A, \underline{\mathbf{x}}_B) = \Psi_0^A(\underline{\mathbf{x}}_A) \, \Psi_0^B(\underline{\mathbf{x}}_B) \sqrt{1 + \sum_{i \in A, j \in B} J_R(\mathbf{r}_i, \mathbf{r}_j)} \tag{3}$$

where the function $J_R$ correlates electrons in $A$ with those in $B$ and is written in the form

$$J_R(\mathbf{r}, \mathbf{r}') = \sum_{ij} c_{ij,R} b_i^A(\mathbf{r}) \, b_j^B(\mathbf{r}') \tag{4}$$

where $c_{ij,R}$ are parameters, which are determined variationally. The functions $b_i^{A/B}(\mathbf{r})$ for now are an arbitrary set of "dispersals," used as basis to expand $J_R$. The constraint $\Psi_R \to |\Psi_0^A|^2$, $|\Psi_0^B|^2$ is enforced by imposing[4]

$$\int \rho_0^A(\mathbf{r}_{i_A}) \, J_R(\mathbf{r}_{i_A}, \mathbf{r}_{j_B}) \, d\mathbf{r}_{i_A} = 0 \quad \forall \, \mathbf{r}_{j_B} \tag{5}$$

$$\int \rho_0^B(\mathbf{r}_{j_B}) \, J_R(\mathbf{r}_{i_A}, \mathbf{r}_{j_B}) \, d\mathbf{r}_{j_B} = 0 \quad \forall \, \mathbf{r}_{i_A} \tag{6}$$

Thanks to this constraint, the expectation of the external potential and that of the electron−electron interactions inside each monomer cancel out in the interaction energy, whose variational minimization takes a simplified form.[4,7] If we peform the multipolar expansion of the monomer−monomer interaction, we can, accordingly, expand $c_{ij,R}$ in a series of inverse powers of $R$:

$$c_{ij,R} = c_{ij}^{(3)} R^{-3} + c_{ij}^{(4)} R^{-4} + c_{ij}^{(5)} R^{-5} + O(R^{-6}) \tag{7}$$

which leads to explicit expressions for the dispersion coefficients. In this paper, we focus on the leading $C_6$ coefficient of the term $-C_6 R^{-6}$ in the dispersion interaction energy, which is determined by the variational parameters $c_{ij}^{(3)}$ in eq 7, denoted simply $c_{ij}$ in the rest of this work.

As detailed in the Supporting Information of ref 4, the variational equation for $C_6$ corresponding to our wave function is given in terms of the matrices $\tau_{ij}^{A/B}$, $S_{ij}^{A/B}$, and $P_{ij}^{A/B}$ (which determine the kinetic correlation energy)

$$\tau_{ij}^A = \int \rho_0^A(\mathbf{r}) \, \nabla b_i^A(\mathbf{r}) \cdot \nabla b_j^A(\mathbf{r}) \, d\mathbf{r} \tag{8}$$

$$S_{ij}^A = \int \rho_0^A(\mathbf{r}) \, b_i^A(\mathbf{r}) \, b_j^A(\mathbf{r}) \, d\mathbf{r} \tag{9}$$

$$P_{ij}^A = \int d\mathbf{r}_{1_A} \int d\mathbf{r}_{2_A} \, P_0^A(\mathbf{r}_{1_A}, \mathbf{r}_{2_A}) \, b_i^A(\mathbf{r}_{1_A}) \, b_j^A(\mathbf{r}_{2_A}) \tag{10}$$

with similar expressions for system $B$, and of the matrix $w_{ij}$ (which determines the monomer−monomer interaction)

$$w_{ij} = \sum_{e=x,y,z} h_e(d_{e,i}^A + D_{e,i}^A)(d_{e,j}^B + D_{e,j}^B) \tag{11}$$

with $e = x, y, z$, and $h_e = (1, 1, -2)$ when the intermolecular axis is parallel to the $z$-axis. The vectors $\mathbf{d}_i^A$ and $\mathbf{D}_i^A$ determine the dipole−dipole interaction terms:

$$\mathbf{d}_i^A = \int d\mathbf{r}_{1_A} \, \rho_0^A(\mathbf{r}_{1_A}) \, b_i^A(\mathbf{r}_{1_A}) \mathbf{r}_{1_A} \tag{12}$$

$$\mathbf{D}_i^A = \int d\mathbf{r}_{1_A} \int d\mathbf{r}_{2_A} \, P_0^A(\mathbf{r}_{1_A}, \mathbf{r}_{2_A}) \, b_i^A(\mathbf{r}_{2_A}) \mathbf{r}_{1_A} \tag{13}$$

with, again, similar expressions for monomer $B$. In eqs 10 and 13 $P_0^{A/B}$ is the ground-state pair density of the two monomers, with usual normalization to $N(N-1)$.

In our previous work[4] the matrices $S_{ij}^{A/B} + P_{ij}^{A/B}$ were diagonalized through a Löwdin orthogonalization among the $b_i$, transforming the matrices $w_{ij}$ and $\tau_{ij}^{A/B}$ accordingly. The variational coefficients $c_{ij}$ were then determined via the solution of a Sylvester equation:[4,17]

$$\sum_k \tau_{ik}^A c_{kj} + \sum_l c_{il} \tau_{lj}^B = -4w_{ij} \tag{14}$$

Here we diagonalize $\tau_{ij}^{A/B}$ with $S_{ij}^{A/B} + P_{ij}^{A/B}$ as a metric through a generalized eigenvalue problem, again transforming accordingly $w_{ij}$, so the indices indicate from now on matrix elements with the transformed $b_i$. The advantage is that this eigenvalue problem needs to be solved only once for each monomer, while the Sylvester equation, eq 14, needs to be solved for each pair $AB$. This way we can directly obtain the variational coefficients $c_{ij}$ as

$$\sum_k \delta_{ik} \tau_i^A c_{kj} + \sum_l \delta_{jl} \tau_j^B c_{il} = 4w_{ij} \tag{15}$$

$$\tau_i^A c_{ij} + \tau_j^B c_{ij} = 4w_{ij} \tag{16}$$

and

$$c_{ij} = -\frac{4w_{ij}}{\tau_i^A + \tau_j^B} \tag{17}$$

The dispersion coefficient $C_6$ then takes the simpler (and computationally faster) form

$$C_6^{AB} = -\sum_{ij} c_{ij} w_{ij} - \frac{1}{8} \sum_{ij} c_{ij}^2 (\tau_i^A + \tau_j^B) = \sum_{ij} \frac{2w_{ij}^2}{\tau_i^A + \tau_j^B} \tag{18}$$

For molecules, eq 18 gives access to the orientation-dependent $C_6^{AB}$ coefficient, where the kinetic energy terms $\tau_i^{A/B}$ are clearly rotationally invariant, and the dependence on the relative orientation of the monomers enters through $w_{ij}$, as shown by eqs 11−13. In order to compare with values from the literature, it is often necessary to compute the orientation-averaged isotropic $\bar{C}_6^{AB}$ coefficients, which can be obtained by performing the orientation average directly on each $w_{ij}^2$, yielding

$$\bar{C}_6^{AB} = \sum_{ij} \frac{2\overline{w_{ij}^2}}{\tau_i^A + \tau_j^B} \tag{19}$$

The $\overline{w_{ij}^2}$ is the spherically averaged interaction term given by

$$\overline{w_{ij}^2} = \frac{2}{3} \sum_{e=x,y,z} (d_{e,i}^A + D_{e,i}^A)^2 \sum_{f=x,y,z} (d_{f,j}^B + D_{f,j}^B)^2 \tag{20}$$

To also assess the accuracy for the orientation dependence, we consider the case of linear molecules, for which one usually defines anisotropic dispersion coefficients by writing the dispersion coefficient $C_6$ as[18]

$$
\begin{aligned}
C_6^{AB}&(\theta_A, \phi_A, \theta_B, \phi_B) \\
&= \bar{C}_6^{AB}\big(1 + \Gamma_6^{AB} P_2(\cos(\theta_A)) + \Gamma_6^{BA} P_2(\cos(\theta_B)) \\
&\quad + \Delta_6^{AB} \frac{4\pi}{5} \sum_{m=-2}^{2} (3 - |m|) Y_2^m(\theta_A, \phi_A) \, Y_2^{-m}(\theta_B, \phi_B)\big)
\end{aligned}
\tag{21}
$$

where $P_n$ denotes Legendre polynomials and $Y_l^m$ denotes spherical harmonics. The anisotropic dispersion coefficients $\Gamma_6^{AB}$ and $\Delta_6^{AB}$ can be obtained from our formalism as

$$\Gamma_6^{AB} = \frac{2}{3\bar{C}_6} \sum_{ij} \frac{-\sum_{e=x,y,z} h_e(d_{e,i}^A + D_{e,i}^A)^2 \sum_{f=x,y,z} (d_{f,j}^B + D_{f,j}^B)^2}{\tau_i + \tau_j} \tag{22}$$

$$\Delta_6^{AB} = \frac{1}{3\overline{C}_6} \sum_{ij} \frac{\sum_{e=x,y,z} h_e (d_{e,i}^A + D_{e,i}^A)^2 \sum_{f=x,y,z} h_f (d_{f,j}^B + D_{f,j}^B)^2}{\tau_i + \tau_j} \tag{23}$$

A similar expression holds for $\Gamma_6^{BA}$, but with the roles of $A$ and $B$ exchanged.

On top of the monomer calculations, the diagonalization to compute $C_6$ scales formally as $n_A{}^3 + n_B{}^3$, where $n_{A/B}$ is the number of dispersals $b_i^{A/B}$ needed to converge, which, however, seems so far independent of system size. We should however also mention the cost of computing the matrix elements: the most expensive part is the first step of the two-step contraction to obtain $P_{ij}$, which scales as $O(N_{orb}{}^4 n_{A/B})$, while the second step scales as $O(N_{orb}{}^2 n_{A/B}{}^2)$, as expensive as obtaining $S_{ij}$ and $\tau_{ij}$, where $N_{orb}$ is the number of spatial orbitals used in the monomer calculations.

## 3. COMPUTATIONAL DETAILS

**3.1. Choice of the Dispersals $b_i(r)$.** For the dispersals $b_i^{A/B}(\mathbf{r})$ of eq 4, we have chosen multipoles centered in $\mathbf{r}_0 = (x_0, y_0, z_0)$:

$$b_i(\mathbf{r}) = (x - x_0)^{s_i}(y - y_0)^{t_i}(z - z_0)^{u_i} \tag{24}$$

For atoms the obvious choice for $\mathbf{r}_0$ is the position of the nucleus; for molecules, in this first exploration, we have set $\mathbf{r}_0$ at the center of nuclear mass. We include all $b_i$ such that $s_i + t_i + u_i < n_{max}$, where $n_{max}^{A/B}$ is a parameter, which is set equal to 22 in all our calculations, which yields in general reasonably converged results (see section 3.5 for a more detailed discussion on convergence). We should remark that the choice of eq 24 is dictated mainly by the immediate availability of integrals: our goal here is to investigate whether the method is worth investing in further implementation and optimization. The question on how to determine the best possible $b_i^{A/B}(\mathbf{r})$ is open, with different strategies discussed in ref 7.

In our previous work,[4,7] the atomic (spherically symmetric) case was also studied in detail. In those calculations a different basis set was used instead of eq 24, namely, a spherical multipole

$$b_i(\mathbf{r}) = r^{l_i + n_i} Y_{l_i m_i}(\theta, \phi) \tag{25}$$

where now the parameters $l_i$, $m_i$, and $n_i$ need to be chosen. This set of spherical multipoles includes the previous (Cartesian) multipoles from eq 24, but also includes cases where $l_i + n_i$ are odd, which are not included in the Cartesian multipoles. The spherical multipole expansion was found to converge faster (sometimes much faster), but it requires nonstandard integrals. Since our purpose here is to test the overall accuracy of the method, we have preferred to use easily available integrals.

**3.2. Matrix Elements.** We denote the spatial orbitals used in the monomer calculations by $\phi_a(\mathbf{r})$ with indices $a$, $b$, $c$, and $d$. The spin-summed one-body reduced density matrix (1-RDM) is written as $\gamma_{ab}$:

$$\gamma(\mathbf{r}, \mathbf{r}') = \sum_{ab} \gamma_{ab} \phi_a(\mathbf{r}) \phi_b(\mathbf{r}') \tag{26}$$

normalized here to $N$. The method only depends on the spatial diagonal $\rho_0(\mathbf{r}) = \gamma(\mathbf{r}, \mathbf{r})$. The 2-RDM is written as $\Gamma_{ab,cd}$, again spin-summed, corresponding to

$$\Gamma(\mathbf{r}_1, \mathbf{r}_2; \mathbf{r}_1', \mathbf{r}_2') = \sum_{abcd} \Gamma_{ab,cd} \phi_a(\mathbf{r}_1) \phi_b(\mathbf{r}_1') \phi_c(\mathbf{r}_2) \phi_d(\mathbf{r}_2') \tag{27}$$

with normalization $N(N-1)$. The method only depends on the spatial diagonal (pair density), $P_0(\mathbf{r}_1, \mathbf{r}_2) = \Gamma(\mathbf{r}_1, \mathbf{r}_2; \mathbf{r}_1, \mathbf{r}_2)$.

To compute the matrix elements of section 2, we need the 1-RDM and 2-RDM of the monomers and the integrals of the dispersals $b_i(\mathbf{r})$ with the spatial orbitals, which, with the choice of eq 24, are all of the kind

$$I_{stu}^{ab} = \int (x - x_0)^s (y - y_0)^t (z - z_0)^u \phi_a(\mathbf{r}) \phi_b(\mathbf{r}) \, d\mathbf{r} \tag{28}$$

For every monomer we need to calculate $S_{ij}$ of eq 9, $\tau_{ij}$ of eq 8, and $\mathbf{d}_i$ of eq 12 from the 1-RDM and $P_{ij}$ of eq 10 and $\mathbf{D}_i$ of eq 13 from the 2-RDM. We first write all the matrix elements by assuming that the constraint of eqs 5 and 6 is satisfied, which amounts to assuming

$$p_i = \frac{1}{N} \int b_i(\mathbf{r}) \rho(\mathbf{r}) \, d\mathbf{r} = \sum_{ab} \frac{\gamma_{ab}}{N} I_{s_i, t_i, u_i}^{ab} = 0 \tag{29}$$

When this does not hold, we make the appropriate modifications in terms of $p_i$; see eqs 36−39 below.

We then have for the matrix $S_{ij}$ of eq 9

$$S_{ij} = \sum_{ab} \gamma_{ab} I_{s_i+s_j, t_i+t_j, u_i+u_j}^{ab} \tag{30}$$

and for $\tau_{ij}$ of eq 8

$$\tau_{ij} = s_i s_j \sum_{ab} \gamma_{ab} I_{s_i+s_j-2, t_i+t_j, u_i+u_j}^{ab} + t_i t_j \sum_{ab} \gamma_{ab} I_{s_i+s_j, t_i+t_j-2, u_i+u_j}^{ab} + u_i u_j \sum_{ab} \gamma_{ab} I_{s_i+s_j, t_i+t_j, u_i+u_j-2}^{ab} \tag{31}$$

The components of the vector $\mathbf{d}_i$ of eq 12 are given by the dipole moment in directions $e = x, y, z$. For example, for the $x$-direction

$$d_{x,i} = \sum_{ab} \gamma_{ab} I_{s_i+1, t_i, u_i}^{ab} \tag{32}$$

while for $y$ and $z$ we get analogous expressions with $I_{s_i, t_i+1, u_i}^{ab}$ and $I_{s_i, t_i, u_i+1}^{ab}$, respectively. For convenience, we also define (with analogous expressions for the $y$- and $z$-directions)

$$d_{x,0} = \int (x - x_0)\rho(\mathbf{r}) \, d\mathbf{r} = \sum_{ab} \gamma_{ab} I_{1,0,0}^{ab} \tag{33}$$

The matrix $P_{ij}$ of eq 10, which is a sort of overlap mediated by the pair density, is given by

$$P_{ij} = \sum_{abcd} \Gamma_{ab,cd} I_{s_i, t_i, u_i}^{ab} I_{s_j, t_j, u_j}^{cd} \tag{34}$$

For the components of the vector $\mathbf{D}_i$ of eq 13 we have, for example, in the $x$-direction

$$D_{x,i} = \sum_{abcd} \Gamma_{ab,cd} I_{1,0,0}^{ab} I_{s_i, t_i, u_i}^{cd} \tag{35}$$

with similar expressions with $I_{0,1,0}^{ab}$ and $I_{0,0,1}^{ab}$ for the other two components. When $p_i$ of eq 29 is not zero, we need to modify the matrix elements according to

$$S_{ij} = \sum_{ab} \gamma_{ab} I_{s_i+s_j, t_i+t_j, u_i+u_j}^{ab} - N p_i p_j \tag{36}$$

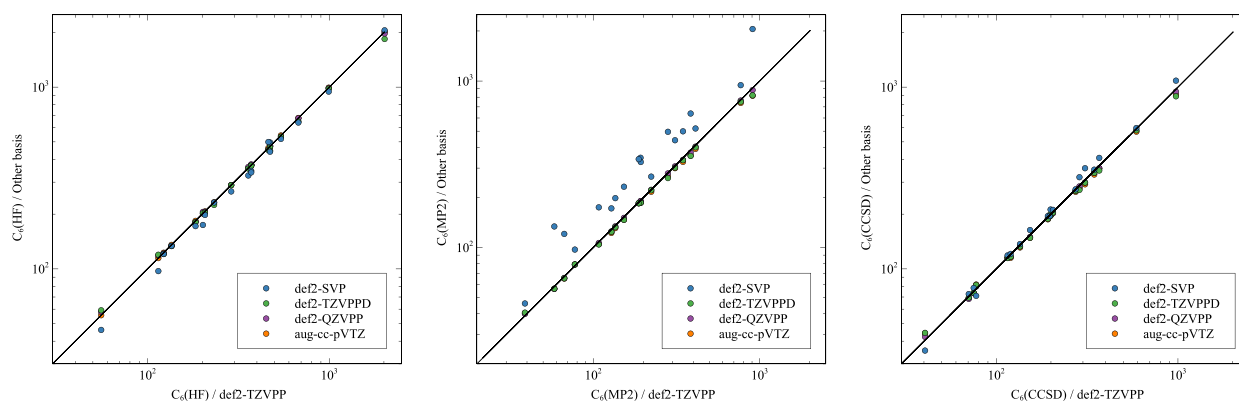$$d_{x,i} = \sum_{ab} \gamma_{ab} I_{s_i+1, t_i, u_i}^{ab} - p_i d_{x,0} \tag{37}$$

**Figure 1.** Isotropic $\overline{C}_6^{AA}$ dispersion coefficients for molecules calculated using Hartree−Fock, MP2, and CCSD pair densities with different basis sets compared with calculations done using def2-TZVPP basis set. Coefficients calculated with the MP2 pair density are the most sensitive to the basis set used, while Hartree−Fock and CCSD methods produce quite robust results. The largest outlier for all the methods used is the $CS_2$ molecule, which is further discussed in section 3.5 and in Figure 2.
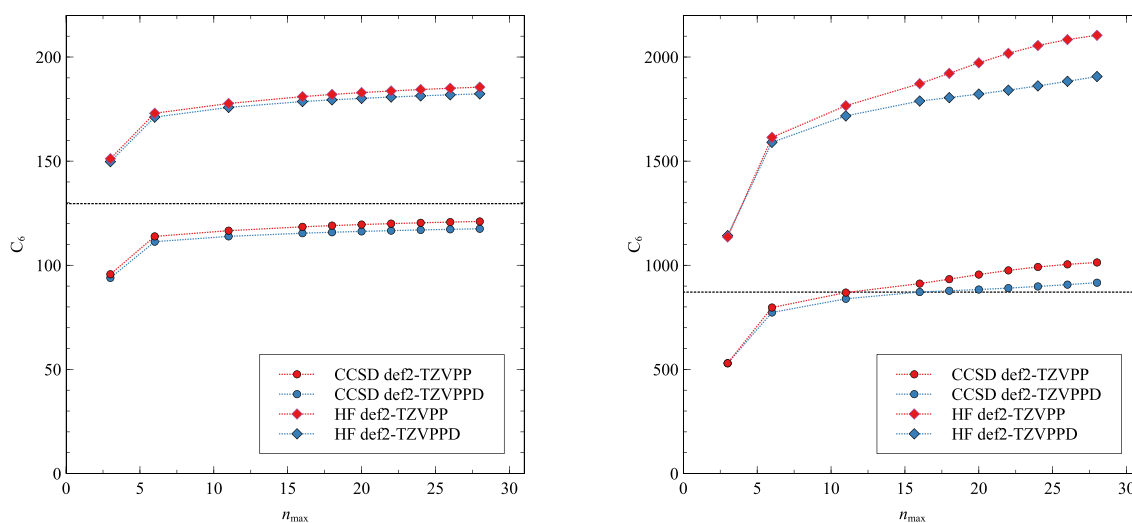


**Figure 2.** Isotropic $\overline{C}_6^{AA}$ coefficients for $CH_4$ (left) and $CS_2$ (right) as a function of $n_{max}$, related to the number of dispersals used to expand the function $J_R(\mathbf{r}, \mathbf{r}')$ of eq 4, for Hartree−Fock and CCSD pair densities of the monomers in different basis sets. Reference values from DOSD measurements are shown with a dotted line. The case of $CH_4$ is representative for what we have observed for the vast majority of systems. $CS_2$ is the worst case found: it is clearly not well converged and needs diffuse functions in the basis set.

$$P_{ij} = \sum_{abcd} \Gamma_{ab,cd} I^{ab}_{s_i,t_i,u_i} I^{cd}_{s_j,t_j,u_j} - p_i p_j N(N-1) \tag{38}$$

$$D_{x,i} = \sum_{abcd} \Gamma_{ab,cd} I^{ab}_{1,0,0} I^{cd}_{s_i,t_i,u_i} - (N-1) p_i d_{x,0} \tag{39}$$

with analogous expressions for the components $y$ and $z$ of $\mathbf{d}_i$ and $\mathbf{D}_i$ and for $d_{x,0}$ defined in eq 33.

**3.3. Implementation.** The expression for the dispersion coefficients of eqs 18 and 19, with the computational details just described, has been written in Python and interfaced with PySCF[19] and HORTON.[20] The Python package is open-source and is available on Github (https://github.com/DerkKooi/fdm). The reduced density matrices of the monomers are obtained from PySCF, and the multipole moment integrals are calculated using HORTON. The monomer densities and pair densities have been computed at three different levels of theory—Hartree−Fock, MP2, and CCSD—where for open-shell systems we used restricted open-shell Hartree−Fock (ROHF). The geometries of the molecules were optimized

using the ORCA program package[21] using the MP2 level of theory with the def2-TZVPPD basis set.

**3.4. Choice of Basis Set for Monomer Calculations.** We have extensively explored the dependence on the basis set used for the monomer pair density calculations for all but the largest molecules, finding that, in general, going beyond a def2-TZVPP (or equivalent) quality does not particularly improve the overall results, with few singular exceptions. The mean absolute percentage errors (MAPEs) for dispersion coefficients of molecules obtained with the def2-QZVPP basis set differ from the def2-TZVPP ones by 1.5−2.2%, with Hartree−Fock being the least and CCSD the most sensitive. When diffuse functions are incorporated into the basis set, the MAPE difference between def2-TZVPP and def2-TZVPPD basis sets ranges from 2.6 to 3.5%, with Hartree−Fock being the least sensitive and MP2 the most sensitive. These differences are less than half the MAPE with respect to the reference values. As a representative example, in Figure 1 we show the $\overline{C}_6^{AA}$ for the molecules considered here with HF, MP2, and CCSD pair densities using different basis sets compared with calculations done using the

def2-TZVPP basis set, which is our choice for all the results presented in section 4.

We should also remark that, since Hartree−Fock pair densities usually lead to an overestimation of $C_6$, if one uses a smaller double-$\zeta$ basis set the performance in this case usually improves as the smaller basis makes the overestimation less profound. The results obtained using a correlated pair density, however, become worse if we go below triple-$\zeta$ quality.

All our results obtained with different basis sets are available in the Supporting Information.

**3.5. Convergence with Respect to Number $n_{max}$ of Dispersals.** In all our calculations we have fixed $n_{max} = 22$, which yields in general well-converged results for the vast majority of cases, and it is also a value for which the multipole integrals are numerically stable. However, we should remark that there are a few cases in which the convergence with the number of $b_i$ has not been satisfactorily reached. As a typical example for how the vast majority of systems behave, we show in the left panel of Figure 2 the convergence of $\overline{C}_6^{AA}$ for $CH_4$ with respect to $n_{max}$, for both HF and CCSD pair densities, with and without diffuse functions in the basis set for the monomer calculation. We see that the result is well converged and that the addition of diffuse functions has little effect, with CCSD underestimating the $C_6$ coefficient. There are however three molecules ($SO_2$, $CS_2$, and $CO_2$) where the values between $n_{max} = 20$ and $n_{max} = 22$ deviate more than 1%. The worst case is $CS_2$, shown in the right panel of Figure 2: we see that even at $n_{max} = 28$ the dispersion coefficient of $CS_2$ is not converged and that CCSD overestimates $C_6$. The inclusion of diffuse functions, in this case, improves both the convergence profile and the accuracy.

## 4. RESULTS

Dispersion coefficients were computed for five data sets:

(1) $C_6^{AA}$ for 23 atoms and ions
(2) $C_6^{AB}$ for 253 mixed pairs consisting of atoms and ions
(3) isotropic $\overline{C}_6^{AA}$ for a set of 26 molecules
(4) isotropic $\overline{C}_6^{AB}$ for a set of 157 mixed molecule pairs
(5) anisotropic $\Gamma_6^{AB}$ and $\Delta_6^{AB}$ (where applicable) for three diatomics and interacting with noble gas atoms

In all cases we compare our results with reference values obtained from dipole oscillator strength distribution (DOSD) data computed[22] or constructed from measurements and theoretical constraints.[18,23−37]

**4.1. Dispersion Coefficients for Atoms and Ions.** The results for set 1, using HF, MP2, and CCSD pair densities (def2-TZVPP basis set, with effective core potential (ECP) for fifth and sixth row elements) for the monomers are presented in Table 1 and compared with accurate reference data.[22] The MAPEs for Hartree−Fock, MP2, and CCSD monomer pair densities are 62.1, 17.7, and 16.2%, respectively. The same results are also illustrated in Figure 3. Notice that the result for H in Table 1 has a small residual error of 1.2% due to the basis set used, since the results for $C_6^{AA}$ (as well as $C_8^{AA}$ and $C_{10}^{AA}$) from our wave function are exact when the exact hydrogenic orbital is used.[4]

For test set 2, the different pairs are formed by selecting $A$ and $B$ from the species listed in Table 1. The results for the dispersion coefficients $C_6^{AB}$ computed using different pair densities for the monomers, again with the def2-TZVPP basis set, are compared to accurate reference values[22] in Figure 4. The MAPEs for Hartree−Fock, MP2, and CCSD are slightly better,

**Table 1. Dispersion Coefficients $C_6^{AA}$ for a Set of Atoms and Ions Computed Using Hartree−Fock, MP2, and CCSD Pair Densities for Monomers with the def2-TZVPP Basis Set, with Effective Core Potential (ECP) for Fifth and Sixth Row Elements**[a]

| species | ref 22 | HF | MP2 | CCSD |
|---|---|---|---|---|
| H | 6.50 | **6.42** | **6.42** | **6.42** |
| Li | 1395.80 | **1024.59** | 1013.58 | 981.77 |
| Na | 1561.60 | **1458.17** | 1400.47 | 1211.02 |
| K | 3906.30 | 4636.05 | **3919.56** | 3034.83 |
| Rb | 4666.90 | 6493.38 | **5207.21** | 3833.89 |
| Cs | 6732.80 | 11244.92 | 7894.26 | **6008.81** |
| Cu | 249.56 | 466.54 | 393.98 | **312.73** |
| Ag | 342.29 | 741.72 | 441.06 | **392.27** |
| Be⁺ | 68.80 | **40.00** | 39.36 | 38.95 |
| Mg⁺ | 154.59 | **120.87** | 115.17 | 109.78 |
| Ca⁺ | 541.03 | **565.94** | 425.62 | 383.40 |
| Sr⁺ | 775.72 | 1040.23 | **667.53** | 623.11 |
| Ba⁺ | 1293.20 | 2284.40 | **1306.28** | 1348.81 |
| Be | 213.41 | 443.51 | 273.87 | **161.69** |
| Mg | 629.59 | 1257.52 | 750.44 | **523.40** |
| Ca | 2188.20 | 5035.02 | **2441.13** | 1809.39 |
| Sr | 3149.30 | 7882.73 | **3508.83** | 2750.55 |
| Ba | 5379.60 | 15037.42 | 6184.94 | **5892.73** |
| He | 1.46 | 1.62 | **1.43** | **1.43** |
| Ne | 6.38 | 6.79 | 5.91 | **6.19** |
| Ar | 64.30 | 96.28 | 54.60 | **58.57** |
| Kr | 129.56 | 211.12 | 110.30 | **122.45** |
| Xe | 285.87 | 537.65 | 221.15 | **275.55** |
| | | HF | MP2 | CCSD |
| MAPE (%) | | 62.1 | 17.7 | 16.2 |
| AMAX (%) | | 179.5 | 57.9 | 43.4 |

[a]For each species, the dispersion coefficient closest to the reference value is in bold font. The mean absolute percentage error (MAPE) as well as the maximum absolute percent deviation (AMAX) for the data set are reported.
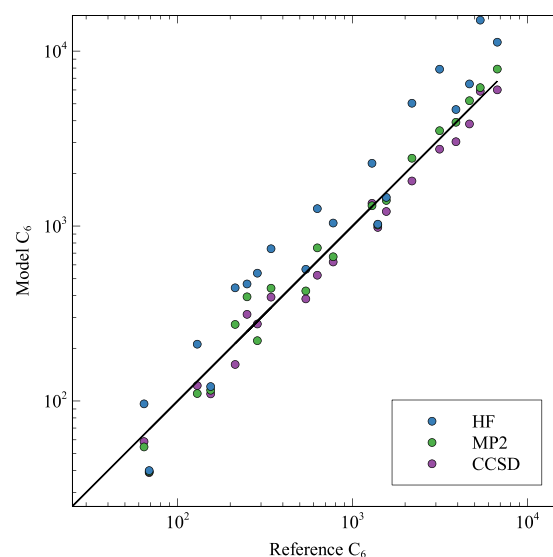


**Figure 3.** Results for $C_6^{AA}$ for 23 atoms and ions (see Table 1). The solid line depicts one-to-one correspondence of the model with the reference data obtained from ref 22. The mean absolute percentage errors for Hartree−Fock, MP2, and CCSD monomer pair densities are 62.1, 17.7, and 16.2%, respectively.

being 52.3, 12.1, and 11.9%, respectively. All the values obtained are available in the Supporting Information.
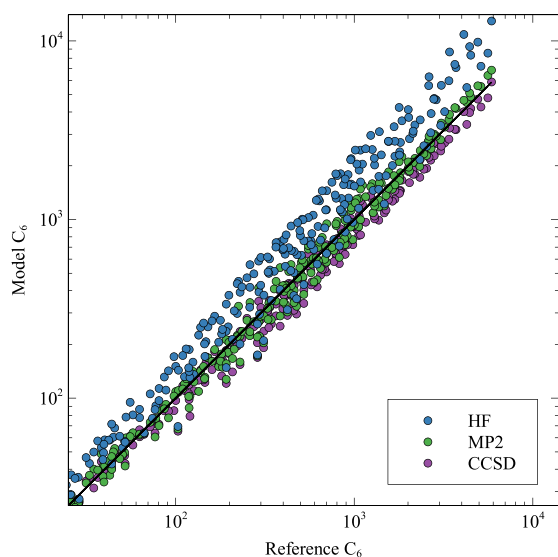


**Figure 4.** Dispersion coefficients $C_6^{AB}$ for 253 pairs formed by selecting A and B from the species listed in Table 1, computed using Hartree–Fock, MP2, and CCSD pair densities for the monomers with the def2-TZVPP basis set. The solid line depicts one-to-one correspondence of the model with the reference data obtained from ref 22. The mean absolute percentage errors for Hartree–Fock, MP2, and CCSD monomer pair densities are 52.3, 12.1, and 11.9%, respectively.

These results for atoms and ions are not extremely promising, in particular because they do not always improve with the accuracy of the theory used to treat the monomers. From Figure 4, it is evident that the use of the Hartree–Fock pair densities leads to an overestimation of the dispersion coefficients. However, for some systems (Li, Na, Be⁺, Mg⁺) the FDM method combined with correlated pair densities considerably underestimates the dispersion coefficient, and in those cases Hartree–Fock pair densities yield better results than MP2 and CCSD ones. As it should, the CCSD pair density tends to produce a lower bound for the dispersion coefficient, but with some exceptions (e.g., Ag, Cu, Ba⁺).

The picture improves considerably if we look at closed-shell species only: if we consider the 15 noble gas pairs, the MAPEs for HF, MP2, and CCSD pair densities are 41.9, 12.2, and 4.3%, respectively. Also, if we consider the subset of our data set formed by the 45 pairs of the noble gas and alkali elements used by Becke and Johnson[11] in their original paper on the exchange-hole dipole moment (XDM) dispersion model (see their Table 1), we obtain MAPEs for MP2 and CCSD equal to 9.6 and 7.7%, respectively, lower than the one of XDM (11.4%), while with Hartree–Fock pair densities our MAPE is 27.3%.

Overall, these first results indicate that the constrained FDM ansatz can work well for closed-shell species, while being less reliable for open-shell cases. As we shall see in section 4.2, the results for the isotropic dispersion coefficients for closed-shell molecules are reasonably accurate and robust, confirming these first findings.

### 4.2. Isotropic Dispersion Coefficients for Molecules.
Isotropic molecular dispersion coefficients $\overline{C}_6^{AA}$ were computed for 26 molecules consisting mainly of first and second row elements. Our results are compared with reference values

calculated from DOSD[23−36] in Table 2 and are also illustrated in Figure 5. The MAPE using Hartree–Fock pair density with

**Table 2. Isotropic Dispersion Coefficients $\overline{C}_6^{AA}$ for a Set of Molecules Calculated Using def2-TZVPP Basis Set[a]**

| species | ref | HF | MP2 | CCSD |
|---|---|---|---|---|
| $H_2$ | 12.1[23] | 16.42 | 15.76 | **11.60** |
| $C_2H_6$ | 381.9[24] | 542.19 | **411.68** | 346.17 |
| $C_2H_4$ | 300.2[35] | 472.25 | **310.09** | 273.50 |
| $C_2H_2$ | 204.1[29] | 372.13 | **192.44** | 192.34 |
| $H_2O$ | 45.3[23] | 55.57 | 38.88 | **40.55** |
| $H_2S$ | 216.8[28] | 358.57 | 193.01 | **199.08** |
| $NH_3$ | 89[23] | 114.66 | **77.58** | 77.52 |
| $SO_2$ | 293.9[26] | 473.00 | 281.11 | **287.00** |
| $SiH_4$ | 343.9[33] | 462.54 | **346.18** | 308.09 |
| $N_2$ | 73.3[23] | 135.53 | 58.37 | **70.57** |
| HF | 19[27] | 21.70 | 16.67 | **17.66** |
| HCl | 130.4[27] | 201.66 | 108.00 | **115.47** |
| HBr | 216.6[27] | 372.17 | 187.65 | **205.25** |
| $H_2CO$ | 165.2[38] | 207.04 | **135.75** | 135.13 |
| $CH_4$ | 129.6[24] | 183.70 | **128.52** | 120.00 |
| $CH_3OH$ | 222[34] | 288.75 | **223.07** | 196.93 |
| $CS_2$ | 871.1[26] | 2017.72 | **906.90** | 975.32 |
| CO | 81.4[39] | 122.69 | 66.98 | **75.13** |
| $CO_2$ | 158.7[39] | 232.44 | 153.00 | **153.45** |
| $Cl_2$ | 389.2[30] | 676.48 | **384.86** | 368.85 |
| $C_3H_6$ | 662.1[35] | 993.49 | 769.43 | **590.50** |
| $C_3H_8$ | 768.1[24] | 1092.09 | 919.72 | **688.07** |
| $C_4H_8$ | 1130.2[35] | 1699.13 | 1527.79 | **1023.72** |
| $C_4H_{10}$ | 1268.2[24] | 1821.45 | 1714.29 | **1137.31** |
| $C_5H_{12}$ | 1905.0[24] | 2733.69 | 2872.35 | **1695.39** |
| $C_6H_6$ | 1722.7[29] | 3116.90 | 2148.87 | **1630.94** |
|  |  | HF | MP2 | CCSD |
| MAPE (%) |  | 52.1 | 13.7 | 8.6 |
| AMAX (%) |  | 131.6 | 50.8 | 18.2 |

[a]For each species, the dispersion coefficient closest to the reference value is in bold font.

def2-TZVPP basis is 52.5%. This comes down to 13.7 and 8.6% when MP2 and CCSD pair densities, respectively, are used. This is in line with the results for the noble gas atoms: there is now a clear systematic improvement with the level of theory of the monomer pair densities, with CCSD yielding good results with the lowest variance.

For test set 4, we have computed isotropic dispersion coefficients $\overline{C}_6^{AB}$ for 157 mixed molecule pairs selected from Table 2. The results are illustrated in Figure 6 where they are compared, again, with reference values from DOSD measurements[23−36] and are available in the Supporting Information. The MAPEs using Hartree–Fock, MP2, and CCSD pair densities are 57.1, 7.9, and 7.2%, respectively.

From these calculations we can confirm that, for closed-shell molecules, the Hartree–Fock pair density leads to consistent overestimation of the dispersion coefficients. The use of a correlated pair density (MP2 or CCSD) improves the results considerably, with CCSD providing better accuracy and lowest scattering of the results. For CCSD, 11 of the 26 $\overline{C}_6^{AA}$'s deviate from the reference value by more than 10%, compared to 16 for MP2 and 26 for Hartree–Fock. With the exception of $H_2CO$, all the CCSD values are within 13% of the reference value.

Regarding the FDM results with Hartree–Fock pair densities, we should stress that in this work we are testing the formalism as
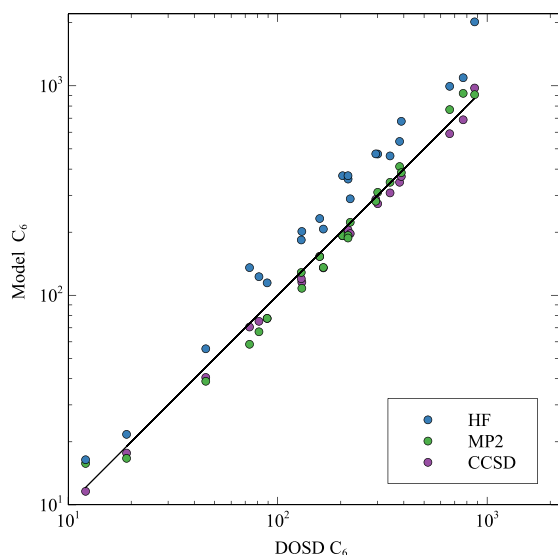
**Figure 5.** Isotropic dispersion coefficients $\overline{C}_6^{AA}$ for molecules calculated using Hartree–Fock, MP2, and CCSD pair densities and reported in Table 2. The solid line depicts one-to-one correspondence of the model with the reference values.
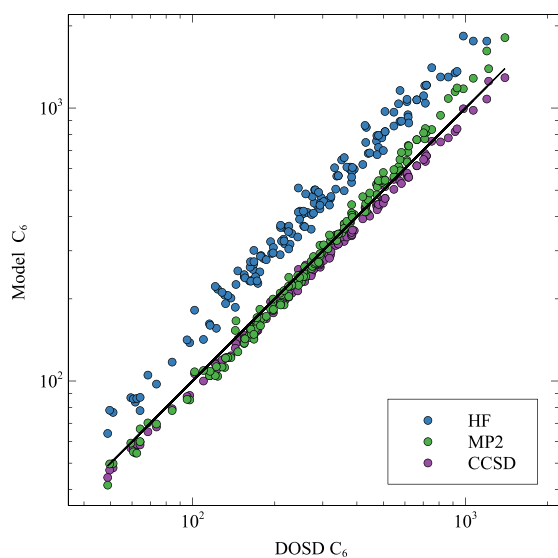


**Figure 6.** Isotropic dispersion coefficients $\overline{C}_6^{AB}$ for 157 mixed molecule pairs selected from Table 2 calculated using Hartree–Fock (MAPE 57.1%), MP2 (MAPE 7.9%), and CCSD (MAPE 7.2%) monomer pair densities (def2-TZVPP basis set). The solid line depicts one-to-one correspondence of the model with the reference values.

derived by our trial FDM wave function when we assume that an exact description of the monomers is used.[4,7] However, if we use Hartree–Fock wave functions for the monomers, we could also revise the formalism to take into account that, in Hartree–Fock theory, part of the intramonomer electron–electron interaction is described in terms of the off-diagonal elements of the one-body reduced density matrix (1-RDM), which do change in the FDM and are quadratic in the variational parameters, such as the kinetic energy. This and other flavors of approximations using Kohn–Sham orbitals and DFT exchange–correlation holes will be extensively tested in future works.

**4.3. Anisotropic Dispersion Coefficients.** To test the applicability of the method for the orientation dependence (anisotropy) of the dispersion coefficients, we performed calculations for the diatomics $H_2$, $N_2$, and CO and for these diatomics interacting with noble gas atoms. The resulting $\Gamma_6^{AB}$ values are listed in Table 3, and the resulting $\Delta_6^{AB}$ values are listed

**Table 3. Anisotropic Dispersion Coefficients $\Gamma_6^{AB}$ for Diatomics $H_2$, $N_2$, and CO and for the Diatomics Interacting with Noble Gas Atoms Calculated Using def2-TZVPP Basis Set**[a]

| pair | ref | HF | MP2 | CCSD |
|------|-----|-----|-----|------|
| $H_2$–$H_2$ | 0.1006[18] | 0.1416 | 0.1099 | **0.1021** |
| $H_2$–$N_2$ | 0.1109[18] | 0.1350 | **0.1040** | 0.0972 |
| $N_2$–$H_2$ | 0.0966[18] | 0.1884 | 0.0474 | **0.1251** |
| $N_2$–$N_2$ | 0.1068[18] | 0.1809 | 0.0442 | **0.1211** |
| $H_2$–He | 0.0924[18] | 0.1288 | 0.1013 | **0.0947** |
| $H_2$–Ne | 0.0901[18] | 0.1240 | 0.0981 | **0.0920** |
| $H_2$–Ar | 0.0971[18] | 0.1343 | 0.1046 | **0.0977** |
| $H_2$–Kr | 0.0986[18] | 0.1369 | 0.1059 | **0.0990** |
| $H_2$–Xe | 0.1005[18] | 0.1397 | 0.1078 | **0.1006** |
| $N_2$–He | 0.1027[18] | 0.1738 | 0.0429 | **0.1192** |
| $N_2$–Ne | 0.0999[18] | 0.1672 | 0.0412 | **0.1164** |
| $N_2$–Ar | 0.1074[18] | 0.1800 | 0.0446 | **0.1214** |
| $N_2$–Kr | 0.1087[18] | 0.1827 | 0.0452 | **0.1223** |
| $N_2$–Xe | 0.1104[18] | 0.1856 | 0.0461 | **0.1234** |
| CO–CO | 0.094[37] | 0.1013 | 0.0600 | **0.0956** |
| CO–$H_2$ | 0.0949[37] | 0.1030 | 0.0616 | **0.0970** |
| $H_2$–CO | 0.0976[37] | 0.1350 | 0.1047 | **0.0979** |
| CO–$N_2$ | 0.0939[37] | 0.1014 | 0.0598 | **0.0954** |
| $N_2$–CO | 0.1077[37] | 0.1808 | 0.0446 | **0.1216** |
| CO–He | 0.093[37] | 0.0997 | 0.0591 | **0.0947** |
| CO–Ne | 0.0916[37] | 0.0975 | 0.0580 | **0.0933** |
| CO–Ar | 0.0942[37] | 0.0975 | 0.0600 | **0.0955** |
| CO–Kr | 0.0943[37] | 0.1016 | 0.0603 | **0.0958** |
| CO–Xe | 0.0944[37] | 0.1021 | 0.0608 | **0.0961** |
| | | HF | MP2 | CCSD |
| MAPE (%) | | 111.1 | 40.3 | 6.9 |
| AMAX (%) | | 213.7 | 67.3 | 23.1 |

[a]For each species, the coefficient closest to the reference value is in bold font. The MAPE and AMAX are calculated for the product $C_6\Gamma_6^{AB}$.

in Table 4. For both $\Gamma_6^{AB}$ and $\Delta_6^{AB}$ CCSD (MAPE 6.9 and 7.4%, respectively) performs better than MP2 (MAPE 40.3 and 58.9%), which in turn performs better than Hartree–Fock (MAPE 111.1 and 210.2%). MP2 performs better for the pairs involving $H_2$ than for the pairs involving $N_2$ and CO.

## 5. CONCLUSIONS AND PERSPECTIVES

The "fixed-diagonal matrices" (FDM) idea[4,7] provides a framework to build new approximations for the dispersion energy in terms of the ground-state pair densities (or the exchange–correlation holes) of the monomers, without the need for polarizabilities. The underlying supramolecular wave function describes a simplified physical mechanism for dispersion, in which only the kinetic energies of the monomers can change. While this is not what happens in the exact case, where all the terms in the isolated monomer Hamiltonian change with respect to their ground-state values, for one-electron fragments the FDM still provides the exact second-order Rayleigh–Schrödinger dispersion energy.[4,7] The purpose

**Table 4. Anisotropic Dispersion Coefficients $\Delta_6^{AB}$ for the Diatomics $H_2$, $N_2$, and CO Calculated Using def2-TZVPP Basis Set**[a]

| pair | ref | HF | MP2 | CCSD |
|---|---|---|---|---|
| $H_2-H_2$ | 0.0108[18] | 0.0214 | 0.0128 | **0.0110** |
| $H_2-N_2$ | 0.0114[18] | 0.0269 | 0.0053 | **0.0126** |
| $N_2-N_2$ | 0.0121[18] | 0.0346 | 0.0021 | **0.0151** |
| CO−CO | 0.0090[37] | 0.0104 | 0.0037 | **0.0092** |
| CO−$H_2$ | 0.0094[37] | 0.0142 | 0.0066 | **0.0096** |
| CO−$N_2$ | 0.0103[37] | 0.0188 | 0.0028 | **0.0118** |
| | | HF | MP2 | CCSD |
| MAPE (%) | | 210.2 | 58.9 | 7.4 |
| AMAX (%) | | 427.0 | 85.9 | 19.8 |

[a]For each species, the coefficient closest to the reference value is in bold font. The MAPE and AMAX are calculated for the product $C_6\Delta_6^{AB}$.

of this work was to investigate how accurate the FDM description can be for systems beyond the simple H and He cases when a good pair density of the monomers is used, focusing on the $C_6$ dispersion coefficients. In the present implementation the computational cost of the step needed on top of the monomers' ground-state calculation is $O(N^4)$.

We have found that for closed-shell species FDM yields rather accurate isotropic dispersion coefficients when CCSD (or even MP2) monomer pair densities are used, with a mean absolute percentage error (MAPE) for CCSD for the whole closed-shell data set (all noble gas atoms and molecule pairs, summarized in Figure 7) of 7.1% and a maximum absolute error (AMAX) within 18.2%. FDM on top of CCSD ground states also predicts the anisotropy of dispersion coefficients, which on a limited set of pairs involving diatomics and noble gas atoms yields satisfactory results for the anisotropy $\Gamma_6^{AB}$ (MAPE 6.9%,
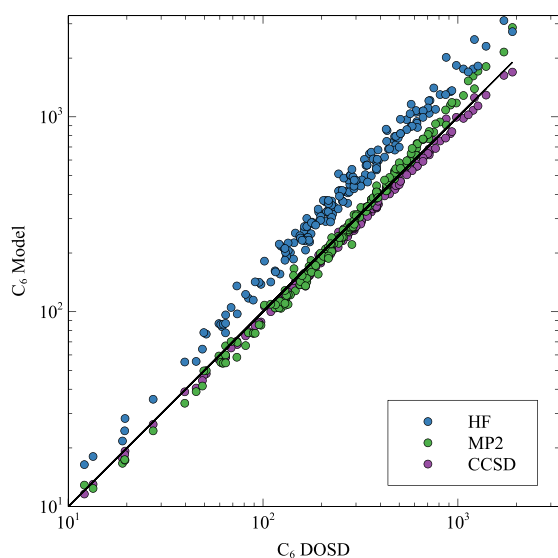


**Figure 7.** Isotropic dispersion coefficients for the whole closed-shell data sets (all molecules and noble gas atoms) calculated using Hartree−Fock (MAPE 55.3%, AMAX 131.6%), MP2 (MAPE 8.9%, 50.78%), and CCSD (MAPE 7.1%, AMAX 18.2%) monomer pair densities (def2-TZVPP basis set). The solid line depicts one-to-one correspondence of our FDM method with the reference values.

AMAX 23.1%) and the anisotropy $\Delta_6^{AB}$ (MAPE 7.4%, AMAX 19.8%).

From this study it also emerged that the basis set used in the monomer calculations has little effect on the computed dispersion coefficients, as the results are essentially converged at the triple-$\zeta$ level. Although not competitive with linear-response (LR) CCSD based methods at the complete basis set (CBS) limit, which can achieve accuracies[40,41] of 1−3%, FDM combined with CCSD pair densities seems to have similar accuracies (for closed-shell systems) of LR CCSD based methods when triple- or double-$\zeta$ basis sets are used for the latter.[40,42] From the data available, the FDM dispersion coefficients calculated by using CCSD pair densities also outperform XDM for both atoms[11] and molecules.[43] The DFT-D4 dispersion model[44] has a notably lower MAPE for a test set consisting of closed-shell molecules, i.e., test sets 3 + 4, but a higher AMAX (MAPE 4.3%, AMAX 29.1%). Other methods such as TS[45] and LRD[46] have also a similar or slightly better performance than FDM with CCSD. The TD-DFT results for all atoms and ions reported by Gould and Bucko[47] can achieve an accuracy between 1 and 5%, and the more refined MCLF method of Manz et al.[48] has again a MAPE of 4.5% for a set of closed-shell molecules. An advantage over methods like DFT-D4 is that FDM also predicts the anisotropy of dispersion coefficients and gives access not only to energetics but also to a wave function that can be used in various frameworks, for example, in a QM/MM setting to model the interaction between the QM and MM parts.[14−16] We should also remark that the performance of our method is less satisfactory for open-shell atoms and ions.

The main motivation for this work is to provide a solid basis for constructing DFT and other approximations based on a microscopic real-space mechanism for dispersion, given by a simple competition between kinetic energy and intermonomer interaction. Before making approximations for the monomers' description, it was important to assess how accurate the method can be when good pair densities are used. Considering that the FDM is parameter-free and does not use the polarizabilities as input, the results for closed-shell systems are satisfactory, indicating that the simplified physical mechanism behind it, although not exact, is a reasonable approximation. In our view, this is also conceptually interesting, as it indicates that it is possible to describe reasonably well the overall rise in energy of the monomers with kinetic-energy-only effects.

In future works we will investigate possible ways to improve the results for open-shell fragments, and we will work on building approximations based on model exchange−correlation holes from density functional theory but also on revisiting the formalism in the Hartree−Fock framework by taking into account the effects of the change in the off-diagonal elements of the 1-RDM on the monomer's Fock operators. We should also stress that the choice of the basis in which to expand the density constraint, i.e., the dispersals $b_i(\mathbf{r})$ of eq 4, is arbitrary and that the current choice of eq 24 is far from optimal. For some cases, the convergence with the number of dispersals is slow, and too-high multipole moment integrals may become numerically unstable. We will thus also explore more closely the determination of an optimal choice for the dispersals as we have preliminary indications[7] that with a proper choice it is possible to use just a few of them to obtain well-converged results.

## ■ ASSOCIATED CONTENT

### ⓢ Supporting Information

The Supporting Information is available free of charge at https://pubs.acs.org/doi/10.1021/acs.jctc.1c00102.

Computed $C_6$ coefficients for the pairs of atoms and ions calculated using various basis sets; isotropic $\overline{C}_6^{AA}$ and $\overline{C}_6^{AB}$ dispersion coefficients for molecule pairs; anisotropic $\Gamma_6^{AB}$ and $\Delta_6^{AB}$ for three diatomics and for the diatomics interacting with noble gas atoms; convergence of HF and CCSD pair densities (XLS)

Descriptions of spreadsheets in Supporting Information (PDF)

## ■ AUTHOR INFORMATION

### Corresponding Authors

**Derk P. Kooi** − *Department of Chemistry & Pharmaceutical Sciences and Amsterdam Institute of Molecular and Life Sciences (AIMMS), Faculty of Science, Vrije Universiteit, 1081HV Amsterdam, The Netherlands;* ⓞ orcid.org/0000-0001-9036-9722; Email: d.p.kooi@vu.nl

**Timo Weckman** − *Department of Chemistry & Pharmaceutical Sciences and Amsterdam Institute of Molecular and Life Sciences (AIMMS), Faculty of Science, Vrije Universiteit, 1081HV Amsterdam, The Netherlands;* Email: t.e.j.weckman@vu.nl

**Paola Gori-Giorgi** − *Department of Chemistry & Pharmaceutical Sciences and Amsterdam Institute of Molecular and Life Sciences (AIMMS), Faculty of Science, Vrije Universiteit, 1081HV Amsterdam, The Netherlands;* ⓞ orcid.org/0000-0002-5952-1172; Email: p.gorigiorgi@vu.nl

Complete contact information is available at:
https://pubs.acs.org/10.1021/acs.jctc.1c00102

### Notes

The authors declare no competing financial interest.

## ■ REFERENCES

(1) Grimme, S.; Hansen, A.; Brandenburg, J. G.; Bannwarth, C. Dispersion-Corrected Mean-Field Electronic Structure Methods. *Chem. Rev.* **2016**, *116*, 5105−5154.

(2) Claudot, J.; Kim, W. J.; Dixit, A.; Kim, H.; Gould, T.; Rocca, D.; Lebègue, S. Benchmarking several van der Waals dispersion approaches for the description of intermolecular interactions. *J. Chem. Phys.* **2018**, *148*, 064112.

(3) Stöhr, M.; Van Voorhis, T.; Tkatchenko, A. Theory and practice of modeling van der Waals interactions in electronic-structure calculations. *Chem. Soc. Rev.* **2019**, *48*, 4118−4154.

(4) Kooi, D. P.; Gori-Giorgi, P. A Variational Approach to London Dispersion Interactions without Density Distortion. *J. Phys. Chem. Lett.* **2019**, *10*, 1537−1541.

(5) Thakkar, A. J. The generator coordinate method applied to variational perturbation theory. Multipole polarizabilities, spectral sums, and dispersion coefficients for helium. *J. Chem. Phys.* **1981**, *75*, 4496−4501.

(6) Korona, T.; Williams, H. L.; Bukowski, R.; Jeziorski, B.; Szalewicz, K. Helium dimer potential from symmetry-adapted perturbation theory calculations using large Gaussian geminal and orbital basis sets. *J. Chem. Phys.* **1997**, *106*, 5109−5122.

(7) Kooi, D. P.; Gori-Giorgi, P. London dispersion forces without density distortion: a path to first principles inclusion in density functional theory. *Faraday Discuss.* **2020**, *224*, 145−165.

(8) Lieb, E. H.; Thirring, W. E. Universal nature of van der Waals forces for Coulomb systems. *Phys. Rev. A: At., Mol., Opt. Phys.* **1986**, *34*, 40−46.

(9) Ángyán, J. G.; Dobson, J.; Jansen, G.; Gould, T. *London Dispersion Forces in Molecules, Solids and Nano-structures: An Introduction to Physical Models and Computational Methods*, 1st ed.; Royal Society of Chemistry: 2020; Chapter 6.

(10) Nguyen, B. D.; Chen, G. P.; Agee, M. M.; Burow, A. M.; Tang, M. P.; Furche, F. Divergence of Many-Body Perturbation Theory for Noncovalent Interactions of Large Molecules. *J. Chem. Theory Comput.* **2020**, *16*, 2258−2273.

(11) Becke, A. D.; Johnson, E. R. Exchange-hole dipole moment and the dispersion interaction. *J. Chem. Phys.* **2005**, *122*, 154104.

(12) Becke, A. D.; Johnson, E. R. Exchange-hole dipole moment and the dispersion interaction revisited. *J. Chem. Phys.* **2007**, *127*, 154108.

(13) Hesselmann, A. Long-range correlation energies from frequency-dependent weighted exchange-hole dipole polarisabilities. *J. Chem. Phys.* **2012**, *136*, 014104.

(14) Giovannini, T.; Lafiosca, P.; Cappelli, C. A General Route to Include Pauli Repulsion and Quantum Dispersion Effects in QM/MM Approaches. *J. Chem. Theory Comput.* **2017**, *13*, 4854−4870.

(15) Giovannini, T.; Ambrosetti, M.; Cappelli, C. Quantum Confinement Effects on Solvatochromic Shifts of Molecular Solutes. *J. Phys. Chem. Lett.* **2019**, *10*, 5823−5829.

(16) Giovannini, T.; Lafiosca, P.; Chandramouli, B.; Barone, V.; Cappelli, C. Effective yet reliable computation of hyperfine coupling constants in solution by a QM/MM approach: Interplay between electrostatics and non-electrostatic effects. *J. Chem. Phys.* **2019**, *150*, 124102.

(17) Bartels, R. H.; Stewart, G. W. Solution of the matrix equation AX ⊕ XB = C [F4]. *Commun. ACM* **1972**, *15*, 820−826.

(18) Meath, W. J.; Kumar, A. Reliable isotropic and anisotropic dipolar dispersion energies, evaluated using constrained dipole oscillator strength techniques, with application to interactions involving H2, N2, and the rare gases. *Int. J. Quantum Chem.* **1990**, *38*, 501−520.

(19) Sun, Q.; Berkelbach, T. C.; Blunt, N. S.; Booth, G. H.; Guo, S.; Li, Z.; Liu, J.; McClain, J. D.; Sayfutyarova, E. R.; Sharma, S. PySCF: the Python-based simulations of chemistry framework. *Wiley Interdiscip. Rev.: Comput. Mol. Sci.* **2018**, *8*, No. e1340.

(20) Verstraelen, T.; Tecmer, P.; Heidar-Zadeh, F.; González-Espinoza, C. E.; Chan, M.; Kim, T. D.; Boguslawski, K.; Fias, S.; Vandenbrande, S.; Berrocal, D.; Ayers, P. W. *HORTON 2.1.1*. 2017. http://theochem.github.com/horton/.

(21) Neese, F. The ORCA program system. *Wiley Interdiscip. Rev.: Comput. Mol. Sci.* **2012**, *2*, 73−78.

(22) Jiang, J.; Mitroy, J.; Cheng, Y.; Bromley, M. Effective oscillator strength distributions of spherically symmetric atoms for calculating polarizabilities and long-range atom−atom interactions. *At. Data Nucl. Data Tables* **2015**, *101*, 158−186.

(23) Zeiss, G.; Meath, W. J. Dispersion energy constants C 6 (A, B), dipole oscillator strength sums and refractivities for Li, N, O, H2, N2, O2, NH3, H2O, NO and N2O. *Mol. Phys.* **1977**, *33*, 1155−1176.

(24) Jhanwar, B.; Meath, W. J. Pseudo-spectral dipole oscillator strength distributions for the normal alkanes through octane and the evaluation of some related dipole-dipole and triple-dipole dispersion interaction energy coefficients. *Mol. Phys.* **1980**, *41*, 1061−1070.

(25) Jhanwar, B.; Meath, W. J. Dipole oscillator strength distributions and properties for methanol, ethanol, and n-propanol. *Can. J. Chem.* **1984**, *62*, 373−381.

(26) Kumar, A.; Meath, W. J. Pseudo-spectral dipole oscillator-strength distributions for SO2, CS2 and OCS and values of some related dipole—dipole and triple-dipole dispersion energy constants. *Chem. Phys.* **1984**, *91*, 411−418.

(27) Kumar, A.; Meath, W. J. Pseudo-spectral dipole oscillator strengths and dipole-dipole and triple-dipole dispersion energy coefficients for HF, HCl, HBr, He, Ne, Ar, Kr and Xe. *Mol. Phys.* **1985**, *54*, 823−833.

(28) Pazur, R.; Kumar, A.; Thuraisingham, R.; Meath, W. J. Dipole oscillator strength properties and dispersion energy coefficients for H2S. *Can. J. Chem.* **1988**, *66*, 615−619.

(29) Kumar, A.; Meath, W. J. Dipole oscillator strength properties and dispersion energies for acetylene and benzene. *Mol. Phys.* **1992**, *75*, 311−324.

(30) Kumar, M.; Kumar, A.; Meath, W. J. Dipole oscillator strength properties and dispersion energies for CI2. *Mol. Phys.* **2002**, *100*, 3271−3279.

(31) Kumar, A. Reliable isotropic dipole properties and dispersion energy coefficients for CCl4. *J. Mol. Struct.: THEOCHEM* **2002**, *591*, 91−99.

(32) Kumar, A.; Kumar, M.; Meath, W. J. Dipole oscillator strengths, dipole properties and dispersion energies for SiF4. *Mol. Phys.* **2003**, *101*, 1535−1543.

(33) Kumar, A.; Kumar, M.; Meath, W. J. Dipole oscillator strength properties and dispersion energies for SiH4. *Chem. Phys.* **2003**, *286*, 227−236.

(34) Kumar, A.; Jhanwar, B.; Meath, W. J. Dipole oscillator strength distributions and properties for methanol, ethanol and propan-1-ol and related dispersion energies. *Collect. Czech. Chem. Commun.* **2005**, *70*, 1196−1224.

(35) Kumar, A.; Jhanwar, B.; Meath, W. Dipole oscillator strength distributions, properties, and dispersion energies for ethylene, propene, and 1-butene. *Can. J. Chem.* **2007**, *85*, 724−737.

(36) Kumar, A.; Meath, W. J. Dipole oscillator strength distributions, properties and dispersion energies for the dimethyl, diethyl and methyl—propyl ethers. *Mol. Phys.* **2008**, *106*, 1531−1544.

(37) Kumar, A.; Meath, W. J. Reliable isotropic and anisotropic dipole properties, and dipolar dispersion energy coefficients, for CO evaluated using constrained dipole oscillator strength techniques. *Chem. Phys.* **1994**, *189*, 467−477.

(38) Kumar, A.; Meath, W. J. Reliable results for the Isotropic Dipole—Dipole and Triple—Dipole Dispersion Energy Coefficients for Interactions involving Formaldehyde, Acetaldehyde, Acetone, and Mono-, Di-, and Tri-Methylamine. *J. Comput. Methods Sci. Eng.* **2004**, *4*, 307−320.

(39) Jhanwar, B.; Meath, W. J. Dipole oscillator strength distributions, sums, and dispersion energy coefficients for CO and CO2. *Chem. Phys.* **1982**, *67*, 185−199.

(40) Korona, T.; Przybytek, M.; Jeziorski, B. Time-independent coupled cluster theory of the polarization propagator. Implementation and application of the singles and doubles model to dynamic polarizabilities and van der Waals constants†. *Mol. Phys.* **2006**, *104*, 2303−2316.

(41) Visentin, G.; Buchachenko, A. A. Polarizabilities, dispersion coefficients, and retardation functions at the complete basis set CCSD limit: From Be to Ba plus Yb. *J. Chem. Phys.* **2019**, *151*, 214302.

(42) Gobre, V. Efficient modelling of linear electronic polarization in materials using atomic response functions. Ph.D. Thesis, Technische Universität Berlin, 2016.

(43) Johnson, E. R.; Becke, A. D. A post-Hartree—Fock model of intermolecular interactions. *J. Chem. Phys.* **2005**, *123*, 024101.

(44) Caldeweyher, E.; Ehlert, S.; Hansen, A.; Neugebauer, H.; Spicher, S.; Bannwarth, C.; Grimme, S. A generally applicable atomic-charge dependent London dispersion correction. *J. Chem. Phys.* **2019**, *150*, 154122.

(45) Tkatchenko, A.; Scheffler, M. Accurate Molecular Van Der Waals Interactions from Ground-State Electron Density and Free-Atom Reference Data. *Phys. Rev. Lett.* **2009**, *102*, 073005.

(46) Sato, T.; Nakai, H. Density functional method including weak interactions: Dispersion coefficients based on the local response approximation. *J. Chem. Phys.* **2009**, *131*, 224104.

(47) Gould, T.; Bučko, T. C6 Coefficients and Dipole Polarizabilities for All Atoms and Many Ions in Rows 1−6 of the Periodic Table. *J. Chem. Theory Comput.* **2016**, *12*, 3603−3613.

(48) Manz, T. A.; Chen, T.; Cole, D. J.; Limas, N. G.; Fiszbein, B. New scaling relations to compute atom-in-material polarizabilities and dispersion coefficients: part 1. Theory and accuracy. *RSC Adv.* **2019**, *9*, 19297−19324.